Overexpression of the Nuclear Receptor Coactivator *AIB1* (*SRC-3*) during Progression of Pancreatic Adenocarcinoma

Ralf Thorsten Henke,[1] Bassem R. Haddad,[1] Sung Eun Kim,[1] Janice Dalby Rone,[1] Aparna Mani,[1] John Milburn Jessup,[1] Anton Wellstein,[1] Anirban Maitra,[2] and Anna Tate Riegel[1]

[1]Department of Oncology, Lombardi Comprehensive Cancer Center, Georgetown University, Washington, DC, and [2]Department of Pathology, Johns Hopkins University School of Medicine, Baltimore, Maryland

ABSTRACT

Purpose: **The nuclear receptor coactivator *amplified in breast cancer 1* (*AIB1*) was found to be amplified and overexpressed in breast and some other epithelial tumors. We have reported that expression of *AIB1* is rate limiting for growth factor, as well as hormone signaling. Here, we assess the involvement of AIB1 in the development of pancreatic adenocarcinoma.**

Experimental Design: **We investigated expression levels of AIB1 protein and mRNA in pancreatic cancer cell lines and in a series of archival pancreatic adenocarcinoma ($n = 78$), pancreatic intraepithelial neoplasia ($n = 93$), pancreatitis ($n = 28$), and normal pancreas tissues ($n = 52$). We also determined *AIB1* gene copy numbers by fluorescence *in situ* hybridization in a subset of cases.**

Results: **In normal pancreas ducts, we rarely found detectable levels of AIB1 mRNA or protein (<6% of the samples). In pancreatitis and low-grade intraepithelial neoplasia, we found an increased frequency of AIB1 expression (>14 and >23%, respectively) relative to normal tissues ($P < 0.01$). Adenocarcinoma, as well as high-grade intraepithelial neoplasia, showed increased levels as well as the highest frequency of AIB1 expression with >65% of samples positive for mRNA and protein ($P < 0.0001$ relative to the other groups). An increased copy number of the *AIB1* gene, observed in 37% of cancers, may account for a portion of the increase in expression.**

Conclusions: **AIB1 overexpression is frequent in pancreatic adenocarcinoma and its precursor lesions. On the basis of its rate-limiting role for the modulation of growth factor signals, we propose a major role of *AIB1* in the multistage progression of pancreatic cancer.**

INTRODUCTION

Pancreatic cancer is the fourth most common cause of cancer-related mortality in the United States, accounting for >30,000 deaths each year (1). The etiology of pancreatic cancer is largely unknown. It is accepted, however, that pancreatic adenocarcinoma arise through multistage progression that initiates in the epithelium of the small interlobular ducts as morphologically distinct lesions known as pancreatic intraepithelial neoplasia or PanIN (2). Several studies have confirmed that genetic changes in PanIN lesions mirror their histologic progression from low-grade to high-grade lesions (2, 3). The identification of novel cellular targets, the expression of which is selectively up-regulated in pancreatic cancers and its precursor lesions, may well enable the early detection of pancreatic cancer in at-risk populations such as patients with inherited pancreatic cancer syndromes (4).

The nuclear receptor coactivator *amplified in breast cancer 1* (*AIB1*) belongs to the p160/steroid receptor coactivator (SRC) family consisting of *SRC-1* (5), *TIF-2* (*GRIP1*; ref. 6) and *AIB1* (ref. 7; *ACTR/RAC3/TRAM-1/SRC-3*) (8–11). The *AIB1* gene is amplified in several human cancers (7, 12–14). *AIB1* enhances the transcriptional activity of a number of nuclear receptors *in vitro* (7, 8, 11) and is rate limiting for estrogen-mediated growth of MCF-7 human breast cancer cells (15). AIB1 overexpression is also positively correlated with the expression of p53 and HER2/neu in breast tumors (16). Disruption of *p/CIP*, the mouse homologue of *AIB1*, results in a pleiotropic phenotype, including reduced female reproductive function and blunted mammary gland development in mice (17, 18). Interestingly, embryonic tissues from *p/CIP*-knockout mice show severe defects in the insulin-like growth factor I and growth hormone signaling pathways (18). Furthermore, an isoform of AIB1 (Δ3-AIB1) that is overexpressed in breast tumors strongly enhances epidermal growth factor-mediated transcription in squamous cell carcinoma cells (19).

Given these data on the emerging role of *AIB1* in human neoplasia, we were interested in determining the expression patterns of AIB1 in pancreatic cancer and in identifying if changes in expression could be correlated with neoplastic progression. Our initial screening revealed high AIB1 protein levels in pancreatic cancer cell lines. Consistent with this, we found nuclear AIB1 highly expressed in human pancreatic adenocarcinoma and also in high-grade PanIN lesions but not in normal

Received 3/22/04; revised 6/4/04; accepted 6/17/04.
Grant support: A grant from the German Department of Education and Research (R. Henke), a Johns Hopkins Clinical Scientist Award (A. Maitra), and grant of the NIH/National Cancer Institute R21 CA108441-01/2 (A. Riegel); the Johns Hopkins tissue microarray facility is supported by a generous grant from the family of Margaret Lee. The costs of publication of this article were defrayed in part by the payment of page charges. This article must therefore be hereby marked *advertisement* in accordance with 18 U.S.C. Section 1734 solely to indicate this fact.
Note: A. Maitra and A. Riegel contributed equally to the direction and oversight of the project.
Requests for reprints: Anna T. Riegel, Georgetown University, LCCC Research Building E307, 3970 Reservoir Road NW, Washington, DC 20057. Phone: (202) 687-1479; Fax: (202) 687-4821; E-mail: ariege01@georgetown.edu.

pancreatic tissue. Furthermore, an increase in *AIB1* gene copy numbers is frequent in pancreatic tumors and likely to be the underlying cause in a subset of pancreatic adenocarcinomas overexpressing AIB1. Thus, selection for AIB1-overexpressing cells represents a frequent and early event in pancreatic tumor development supporting the notion of a growth advantage of cells overexpressing AIB1.

MATERIALS AND METHODS

Cell Lines and Human Tissues. Permission to conduct this study was obtained from the appropriate Institutional Review Boards of the Johns Hopkins University and Georgetown University, respectively.

The pancreatic adenocarcinoma cell line COLO 357 and its sublines L3.6pl and L3.6sl (20) were obtained from Isaiah Fidler (University of Texas M. D. Anderson Cancer Center, Houston, TX). The L3.6pl and L3.6sl cell lines originated from liver metastases in athymic nude mice derived from tumors of COLO 357 cells implanted into the pancreas (L3.6pl) or spleen (L3.6sl; ref. 20).

AIB1 genomic status and AIB1 mRNA and protein expression were examined in normal pancreata ($n = 52$; 19 tumor free organs from autopsies, 33 adjacent normal parenchyma from surgery), chronic pancreatitis ($n = 28$), a spectrum of PanIN lesions ($n = 93$), and invasive pancreatic ductal adenocarcinomas ($n = 78$). A variety of other reference tissues ($n = 147$) were also present in the study, including several samples each of liver, kidney, colon, stomach, brain, lymphatic tissue, lung, prostate hyperplasia, and others. Briefly, formalin-fixed, paraffin-embedded blocks of surgically resected pancreatic adenocarcinomas, PanIN, pancreatitis, and normal pancreata were retrieved from the surgical pathology files of both institutions; additional histologically documented normal autopsy and surgically retrieved pancreata were retrieved from the autopsy archives of Georgetown University. Pancytokeratin immunohistochemistry (IHC) was performed on a subset of cases to prove general protein integrity in autopsy samples. All tissues had been previously processed and successfully used for routine-diagnostic purposes in the according institute. Both facilities used 10% buffered formalin and established protocols for fixation and embedding. The diagnosis was reconfirmed for each case by a gastrointestinal pathologist (A. Maitra). The grades of PanIN lesions were assigned using a previously described classification scheme (2). For the purposes of statistical analysis, PanIN-1A and PanIN-1B were classified as low grade ($n = 72$), and PanIN-2 and PanIN-3 were classified as high grade ($n = 21$), as described previously (21). Regular (full-sized) unstained tissue sections were obtained from the Georgetown University cases, whereas tissue microarrays (TMAs) of pancreatic adenocarcinomas and PanINs were constructed from the Johns Hopkins University cases, as described previously (3, 21). Of the 78 pancreatic adenocarcinoma analyzed, 10 cases were regular sections (Georgetown University) and 68 cases (Johns Hopkins University) were arrayed in a TMA format. It has been shown that TMAs, containing three or more sample cores for each carcinoma, provide results identical to and representative for those obtained from according whole tissue sections (22, 23). We therefore designed our pancreatic adenocarcinoma TMAs with four 1.4-mm cores per tumor; the total number of arrayed adenocarcinoma cores was 272. All PanIN lesions were arrayed, one core per lesion (3, 21); 22 chronic pancreatitis samples were arrayed with 1 to 2 cores each (Hopkins) and 6 were regular sections (Georgetown University). Forty-six of the normal pancreata were present on the cancer and PanIN arrays (Johns Hopkins University) and 6 cases were regular (full-size) sections (Georgetown University).

Western Blotting. COLO 357, L3.6pl, and L3.6sl cells were grown to 70% confluence in DMEM + 10% fetal bovine serum in poly-2-hydroxyethyl methacrylate–coated dishes. Cells were washed with PBS, lysed [50 mmol/L Tris-HCl (pH 8.0), 150 mmol/L NaCl, 40 mmol/L β-glycerophosphate-Na, 0.25% sodium deoxycholate, 1% NP40, 50 mmol/L NaF, 20 mmol/L Na PP_I, 1 mmol/L EGTA, 1 mmol/L Na_3VO_4, 1× Complete Protease Inhibitor (Roche Diagnostics Corp., Indianapolis, IN)], and incubated on ice for 20 minutes. Centrifuged lysates supernatant was boiled in SDS-PAGE buffer with reducing agents. Proteins were resolved by electrophoresis on a 4 to 20% Tris-glycine gel and transferred to a polyvinylidene difluoride membrane. The membrane was blocked for 1 hour with 5% milk/PBST (PBS, 0.2% Tween 20). Antibodies were diluted in 5% milk/PBST and incubated each with the membrane for 1 hour. The following primary antibodies were used: anti-AIB1 (1:250; BD Transduction Laboratories, San Diego, CA) and anti-β-actin (1:3000; Chemicon International, Inc., Temecula, CA). Secondary detection antibodies were part of a commercially available kit (Pierce, New York, NY). Detection was performed with the SuperSignal system (Pierce) and exposure to a photographic film for 5 seconds.

Fluorescence *In situ* Hybridization (FISH). To evaluate the gain of *AIB1* gene copies, we designed a FISH probe consisting of two overlapping bacterial artificial chromosome clones containing sequences of the *AIB1* gene: RP11-109C3 and RP11-456N23 (BACPAC Resources, Oakland, CA). Bacterial artificial chromosome clone DNA was prepared and labeled with Cy3 (Amersham Biosciences, Piscataway, NJ) using nick translation as described previously (24, 25). Correct chromosomal location of the bacterial artificial chromosome clones to chromosome 20q12 was confirmed using standard FISH mapping (24). Metaphase spread chromosomes prepared from the cell lines (COLO 357, L3.6sl, and L3.6pl) and one pancreatic tissue microarray were evaluated by FISH using the *AIB1* probe as described earlier (25). The TMA slide was deparaffinized with xylene, rehydrated with decreasing ethanol concentrations, and pepsin digested for 90 minutes, then denatured in 70% formamide/SSC 2× for 4 minutes at 80°C. After overnight hybridization with the probe at 37°C, the slide was washed three times in formamide/SSC 2× (1:1) at 42°C and three times in SSC 1× at 42°C, then counterstained with 4′,6-diamidino-2-phenylindole and embedded in anti-fade solution [200 mmol/L DABCO (1,4-diazobicyclo[2,2,2]-octane) 90% vol/vol glycerol, 20 mmol/L Tris-HCl (pH 8)] to reduce photo-bleaching.

Scoring of cells and digital image acquisition were performed using a ×63 objective mounted on a Leica DMRBE microscope (Leica, Wetzlar, Germany) equipped with optical filters for 4′,6-diamidino-2-phenylindole and Cy3 (Chroma Technologies, Brattleboro, VT) and a cooled charge coupled device camera (Photometrics, Tucson, AZ). The IPLab software

package (Scanalytics, Inc., Fairfax, VA) was used for the initial gray-scale image acquisition and consecutive color processing. Considering artifacts and loss of genomic contents in partially cut nuclei, the following scoring system was used: FISH signals in 50 cells for each specimen were counted. Detection of three or more signals in at least 30% of the nuclei with detectable signals was considered as increased copy number/gain. In the absence of copy number gain, the presence of two FISH signals per cell in at least 50% of the nuclei was considered as normal diploid.

mRNA Detection by *In situ* Hybridization (ISH). mRNA expression of *AIB1* was assessed by ISH with digoxigenin-labeled riboprobes. A specific 648-bp sequence of the *AIB1* cDNA was subcloned into the pcDNA3 vector (Invitrogen, Carlsbad, CA), and digoxigenin-labeled sense and antisense riboprobes were made from the DNA templates using the DIG RNA labeling kit (Roche Diagnostics Corp.) according to the protocol provided. The probe hybridized with the mRNA of AIB1, as well as the isoform Δ3-AIB1. Tissue slides were stained by ISH using the constructed riboprobes and a previously described protocol (26) with some modifications: in brief, slides were deparaffinized, tissue-proteins were digested with proteinase K, and acetylated (26). The RNA probe was mixed with hybridization solution (1.5 ng probe/1.0 μL solution; Sigma-Aldrich, St. Louis, MO) and incubated with the tissue for 16 to 18 hours at 42°C. Slides were washed and digested with RNase A (Roche Diagnostics Corp.; ref. 26). Refixation and cross-linking was performed by formamide/SSC 2× (1:1) for 10 minutes at 52°C followed by two 5-minute wash steps at 52°C in SSC 1× and SSC 0.5×. After blocking (26), a solution of alkaline-phosphatase–tagged anti-digoxigenin antibody fragments (Roche Diagnostics Corp.) in buffer I [100 mmol/L Tris-HCl (pH 7.5) and 150 mmol/L NaCl] (1:250) was applied and incubated with the tissue for 16 to 18 hours at 4°C. Staining solution was applied, consisting of 0.375 mg/mL nitroblue tetrazolium (Roche Diagnostics Corp.) and 0.175 mg/mL 5-bromo-4-chloro-3-indolyl phosphate (Roche Diagnostics Corp.) diluted in buffer II [100 mmol/L Tris-HCl (pH 9.5), 100 mmol/L NaCl, and 50 mmol/L $MgCl_2$]. Once sufficient staining was observed, the reaction was terminated by rinsing with buffer III [10 mmol/L Tris-HCl (pH 8.0) and 1 mmol/L EDTA] for 10 minutes. Slides were washed in 0.5% Tween 20 and water for 5 minutes each and then allowed to dry completely before mounting with sealing solution and cover slips.

IHC. To investigate AIB1 protein expression we performed IHC as described previously (27). A monoclonal antibody recognizing the amino acids 376–389 of AIB1 (BD Transduction Laboratories) was used as the primary antibody. This antibody also recognizes Δ3-AIB1 (19). Deparaffination and rehydration were performed as detailed for the ISH. The antigen (AIB1) was retrieved by boiling the slides in citrate buffer (pH 6.0) at 100°C for 10 minutes followed by a 20-minute cool down in the solution on the benchtop. Endogenous peroxidase was blocked by 3% H_2O_2 for 10 minutes. Slides were incubated with the primary anti-AIB1 antibody diluted 1:100 in PBS for 16 to 18 hours at 4°C. Detection was performed using the biotin based Super Sensitive detection system (BioGenex, San Ramon, CA) according to the protocol provided. The staining reaction was terminated by rinsing with double-distilled water. Counterstaining of nuclei was performed by 15-second immersion in Mayer hematoxylin. Tissues were dehydrated with increasing concentrations of ethanol and a final immersion in Xylene 100% before the slides were mounted with coverslips.

Evaluation of mRNA and Protein Expression. AIB1 mRNA and protein expression were evaluated in the neoplastic cells of pancreatic adenocarcinoma and in the ductal epithelial cells of PanIN and normal pancreata. Both ISH and IHC results were categorized using identical stratifying criteria for ease of analysis. ISH staining was always evaluated in conjunction with the sense (control) probe. Results were categorized on four different levels: negative (−): signals comparable with sense probe in intensity (ISH), or cytoplasmic, and/or nuclear labeling in <5% of cells (IHC); low positive (+): weak signals unequivocally exceeding sense probe intensity in 5 to 50% of cells (ISH) or cytoplasmic and/or nuclear labeling in 5 to 50% of cells (IHC); positive (++): strong signals in >50% of the cells (ISH) or strong cytoplasmic and/or nuclear labeling in >50% of cells (IHC); and high positive (+++): intense signals in ~100% of cells (ISH) or intense cytoplasmic and/or nuclear labeling in nearly 100% of cells (IHC). The COLO357, 3.6pl, and 3.6sl ISH results and previously stained breast cancer tissue microarrays (data not shown) were also used for comparison during the ISH and IHC evaluation as external controls because AIB1 mRNA and protein expression was known to be present in these samples. Subsequently, this four-tier scheme was converted to a numerical score [ranging from 1 (for negative) to 4 (for +++)] for each examined regular section or tissue microarray core examined. To obtain case results for the cancers with multiple cores on the TMA (68 of the 78 pancreatic adenocarcinoma), we performed additional calculations to consider the heterogeneity of expression frequently observed in adenocarcinoma. We rejected the frequently chosen approach of using only the maximum values of each case to avoid a bias toward high expression results in cancers. Instead mean values were first calculated for each case from all valid core results, resulting in fractional values ranging from 1.00 to 4.00. These were then reassigned to the discrete values 1, 2, 3, and 4 using cutoff values calculated from the statistical distribution of all of the original core values. The resulting recategorized case values had a distribution that was comparable with that of the core values.

Statistical Analysis. Expression results overall tissue-types were compared using the χ^2 test analysis on 5×4 contingency tables. Expression results between pairs of tissue types (normal pancreas, low-grade PanIN, high-grade PanIN, and cancer) were compared with χ^2 test for trend analysis on appropriate 2×4 contingency tables. Correlation of ISH with IHC results was performed by Spearman nonparametric correlation for paired values of the samples; *P* value, correlation coefficient (r), and the 95% confidence interval are given.

RESULTS

AIB1 in Pancreatic Adenocarcinoma Cell Lines. To assess the levels of AIB1 protein expression, we used the cell line COLO 357 and the two metastatic COLO 357 sublines L3.6pl and L3.6sl (20). FISH analysis showed increased copy number of the *AIB1* gene in all three cell lines, where the majority of cells had five to six copies of the gene. A represent-

ative metaphase image for each cell line, evaluated with the *AIB1* FISH probe, is shown in Fig. 1*A*. *In situ* hybridization showed high levels of expression of AIB1 mRNA in the three cell lines and a good signal to noise ratio between the antisense probe and the sense-control (Fig. 1*B*). High levels of the AIB1 protein and the biologically more active isoform Δ3-AIB1 (19) were also detected in all three cell lines by Western blot (Fig. 1*C*).

AIB1 Protein Expression In Tissues, IHC. Aberrant expression of a protein in tumor cell lines may be acquired during passage in culture and may not represent the phenotype of the human tumor. Therefore, to determine the expression pattern ofAIB1 in pancreatic adenocarcinoma, we performed an analysis of the protein and mRNA expression levels in normal pancreata, PanIN, and pancreatic adenocarcinoma. Using IHC, high levels of AIB1 protein were mostly found located in the nuclei of positive neoplastic or adenocarcinoma cells; certain cytoplasmic staining was only present in two normal pancreata and one low grade PanIN. Fig. 2*I* shows a representative example of a high nuclear protein signal with comparably lower

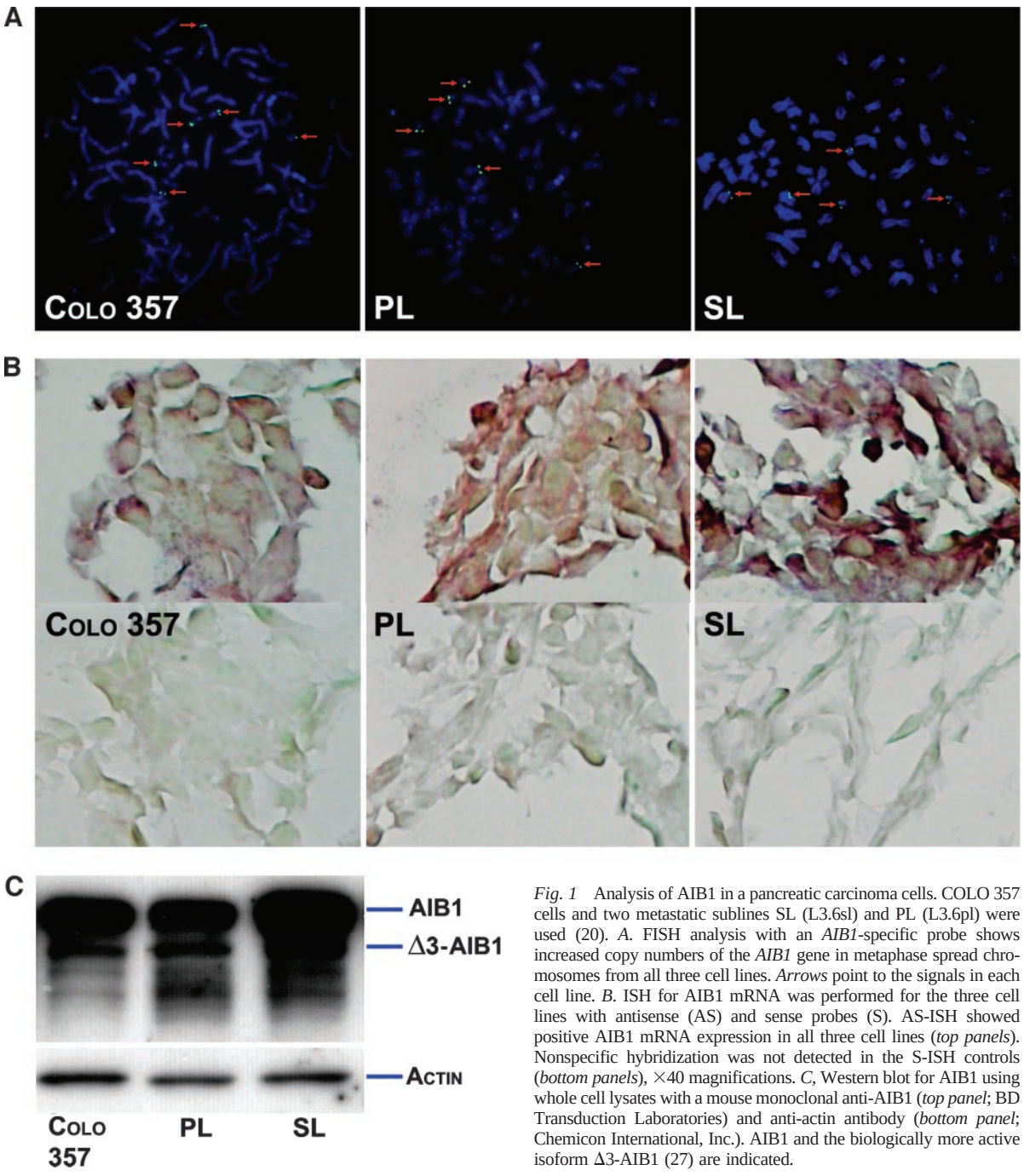

Fig. 1 Analysis of AIB1 in a pancreatic carcinoma cells. COLO 357 cells and two metastatic sublines SL (L3.6sl) and PL (L3.6pl) were used (20). *A.* FISH analysis with an *AIB1*-specific probe shows increased copy numbers of the *AIB1* gene in metaphase spread chromosomes from all three cell lines. *Arrows* point to the signals in each cell line. *B.* ISH for AIB1 mRNA was performed for the three cell lines with antisense (AS) and sense probes (S). AS-ISH showed positive AIB1 mRNA expression in all three cell lines (*top panels*). Nonspecific hybridization was not detected in the S-ISH controls (*bottom panels*), ×40 magnifications. *C,* Western blot for AIB1 using whole cell lysates with a mouse monoclonal anti-AIB1 (*top panel*; BD Transduction Laboratories) and anti-actin antibody (*bottom panel*; Chemicon International, Inc.). AIB1 and the biologically more active isoform Δ3-AIB1 (27) are indicated.

cytoplasmic signal. The control with a nonspecific antibody is shown in Fig. 2*K*. The IHC revealed a significant increase in AIB1 protein expression in the adenocarcinomas and high-grade PanIN lesions when compared with low-grade PanIN lesions, pancreatitis, and normal pancreata (all $P < 0.001$). Representative examples of the IHC staining are shown in the left panels of Fig. 2, and the data are summarized in Table 1 and Fig. 3*B*. Low positive staining (+) was observed in the duct cells of only

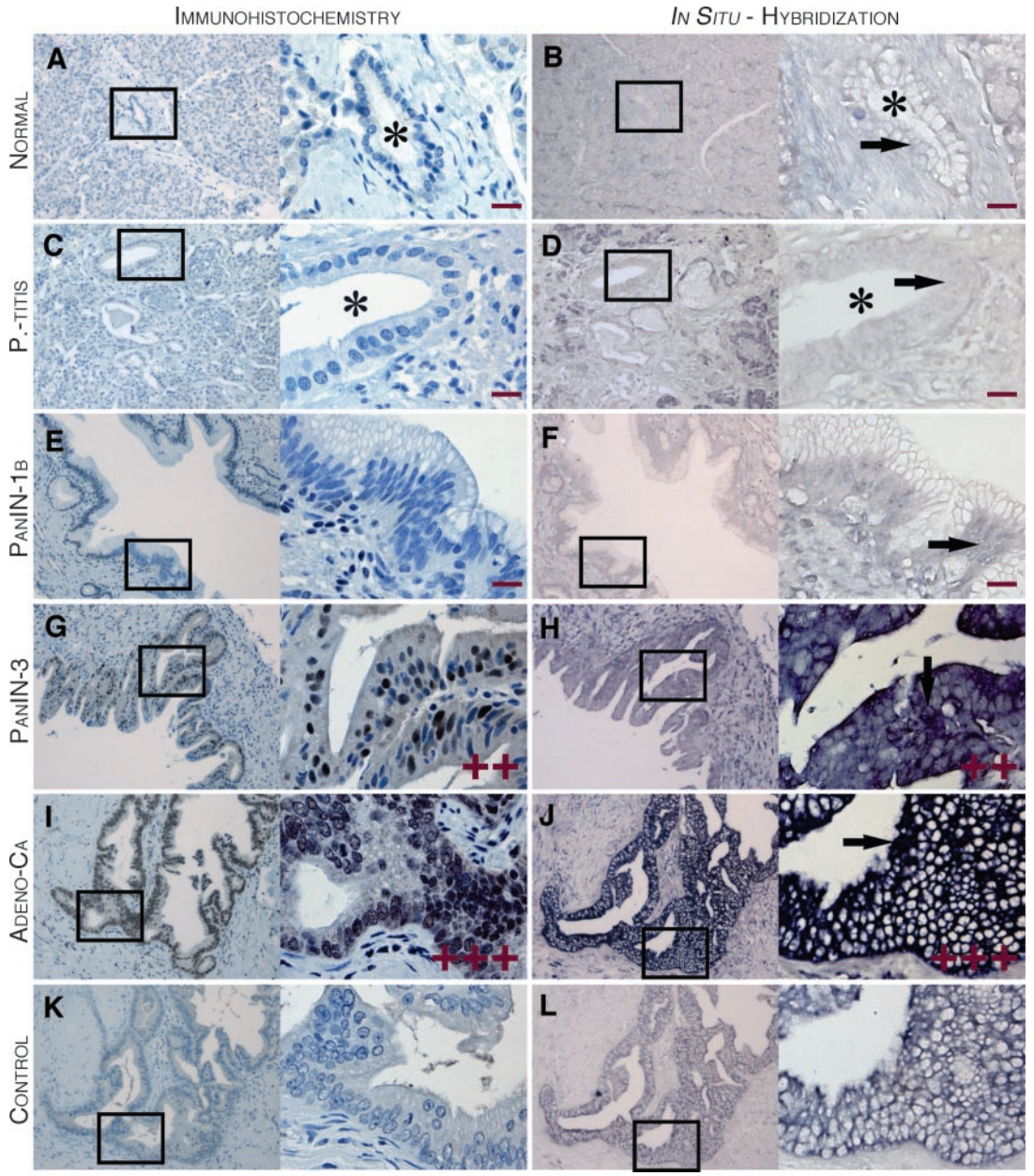

Fig. 2 Examples of AIB1 protein and mRNA expression in pancreatic tissue. TMAs and regular tissue sections were stained for AIB1 protein with IHC using a mouse monoclonal anti-AIB1 antibody (BD Transduction Laboratories) and for mRNA by ISH with digoxigenin-labeled riboprobes. For the IHC, bound anti-AIB1 antibodies were detected with a biotin-avidin-peroxidase system and 3,3′-diaminobenzidine; samples were counterstained with Meyer's hematoxylin. Bound ISH probes were detected by anti-digoxigenin-FAB-alkaline-phosphatase with consecutive NBT/BCIP staining. Results were evaluated for each sample as −, +, ++ or +++. *A–L*. Representative ISH and IHC stainings are shown for different tissues at low (×10 objective) and high (×40 objective) magnification. *Arrows* mark the cytoplasm of appropriate cells. Staining evaluations are given for each case. In both IHC (*A*, *C*, *E*, *G*, and *I*) and ISH (*B*, *D*, *F*, *H*, and *J*), increasing levels and frequencies of AIB1 protein and mRNA were observed with malignant progression. Duct cells of most cases of normal pancreas (*A* and *B*, * = lumen) and pancreatitis (*C* and *D*) showed no staining (−) for both protein and mRNA. *E* and *F*. Most low-grade PanIN were also negative for protein and mRNA but low staining (+) is present in some. *G* and *H*. Most high-grade PanIN had positive staining and high levels (++ and +++) were frequent. Adenocarcinoma (*I* and *J*) had similar high and frequent positive staining. *K* and *L*, controls with a nonspecific antibody (*K*, control for *I*) and sense-mRNA probe (*L*, control for *J*).

2 of 44 cases of normal pancreas tissues. Fifteen of 65 (23.1%) low-grade PanIN and 4 of 28 pancreatitis stained low positive (+). This increase was significant for the low-grade PanIN when compared with normal tissue ($P < 0.01$). A total of 81.0% (17 of 21) of the high-grade PanIN and 64.5% (49 of 76) of the adenocarcinoma showed positive protein expression (+ to +++).

High levels of expression (++ and +++) were frequent in high-grade PanIN and adenocarcinoma but not observed in the normal, pancreatitis, or low-grade PanIN samples. The levels of expression were significantly higher in the adenocarcinoma and the high-grade PanIN when compared with either low-grade PanIN, pancreatitis, or normal tissues (all $P < 0.001$) but not different between the high-grade PanIN and the adenocarcinoma ($P = 0.4$). From these data, we conclude that AIB1 protein levels and frequency increase with progression from normal pancreas via pancreatitis and low-grade to high-grade PanIN and pancreatic adenocarcinoma.

AIB1 mRNA Expression in Tissues, ISH. To study the levels of AIB1 mRNA expression in human tissues, ISH with digoxigenin-labeled RNA probes was performed with adjacent paraffin sections of the same samples that were used for the IHC. Cytoplasmic staining was evaluated according to the grading system used for IHC. For the tissue sections in our study, a distinct pattern of increase in AIB1 mRNA expression was seen in the ISH for high-grade PanIN lesions and adenocarcinoma *versus* normal, pancreatitis, and low-grade PanIN lesions. The results were essentially similar to the IHC. Representative ISH staining in different tissues is shown in the right panels of Fig. 2, and the results are summarized in Table 1*D*. No positive staining was present in the duct cells of the 45 normal pancreata but in 9 of the 25 ducts of pancreatitis. This difference was significant ($P < 0.0001$). Compared with normal duct cells, the lower grade PanIN also showed a significant ($P < 0.0001$) increase in the number of positive cases (43.1%, 28 of 65 cases) but only 2 of these displayed ++ staining. No difference existed between pancreatitis and low-grade PanIN ($P = 0.4$). 75% (15 of 20) of the high-grade PanIN and 73.7% (56 of 76) of the adenocarcinoma displayed positive expression.

Higher levels (++ and +++) of expression were more

Table 1 Tabular overview of staining results

	−	+	++	+++	N/A	*N*	% pos
Immunohistochemistry							
Adenocarcinoma	27	31	15	3	2	78	64.47
High-grade PanIN	4	11	6	0	0	21	80.95
Low-grade PanIN	50	15	0	0	7	72	23.08
Pancreatitis	24	4	0	0	0	28	14.29
Normal pancreas (ducts)	42	2	0	0	8	52	4.55
Other reference tissues	106	6	0	0	35	147	5.36
mRNA *in situ* hybridization							
Adenocarcinoma	20	34	20	2	2	78	73.68
High grade PanIN	5	5	8	2	1	21	75.00
Low grade PanIN	37	26	2	0	7	72	43.08
Pancreatitis	16	9	0	0	3	28	36.00
Normal pancreas (ducts)	45	0	0	0	7	52	0.00
Other reference tissues	114	5	0	1	27	147	5.00

NOTE. N/A, number of samples for which no valid result could be obtained because of missing or necrotic tissues or the lack of the appropriate cell type; *N*, total number of samples; % pos, fraction of samples with +, ++, or +++ expression.

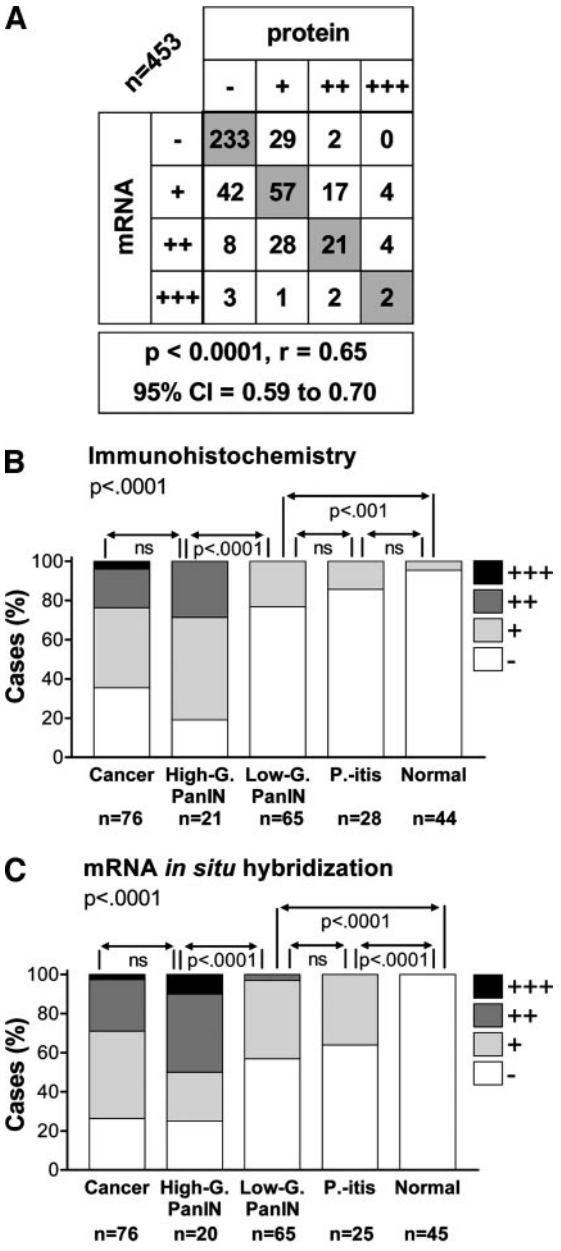

Fig. 3 Analysis of the AIB1 mRNA and protein expression. *A*, correlation of mRNA and protein expression. The numbers of samples for each mRNA and protein expression level are shown. Highlighted fields indicate those with a perfect correlation. r = correlation coefficient, 95% CI = confidence interval. *B* and *C*. ISH and IHC staining distribution are compared between tissue groups using χ^2 test for trend. mRNA and protein expression frequencies at each level are shown in the graph as a percentage. High-G. PanIN = high-grade PanIN (G2 and G3), Low-G. PanIN = Low-grade PanIN (1A and 1B), P.-itis = Pancreatitis. *P* values along the arrows derive from χ^2 test for trend analysis between the indicated tissue types; the *P* values at the top from χ^2 test analysis of all five tissue types. ns = not significant ($P > 0.05$).

frequently observed in the high-grade PanIN and in the adenocarcinoma. These increases in expression levels were significant for both high-grade PanIN and adenocarcinoma when compared with low-grade PanIN, pancreatitis, and normal tissues (all $P < 0.015$, χ^2 test for trend). As observed with the IHC, the expression level distributions were not different between high-grade PanIN and the cancers ($P = 0.2$). We conclude that AIB1 mRNA expression is already increased in half of the cases of early transformation and that it increases additionally in frequency and levels of expression with later progression.

Correlation of AIB1 mRNA and Protein Expression. As mentioned before, consecutive serial sections of the whole tissue and TMA paraffin blocks had been used for IHC and ISH. Therefore, it was possible to correlate the ISH and IHC results directly for each sample. Spearman nonparametric correlation showed a highly significant correlation ($P < 0.0001$, $n = 453$) and a strong correlation coefficient (r) of 0.65 (95% confidence interval, 0.59–0.70). Fig. 3*A* shows all correlated samples as a 4×4 matrix. Cases of mRNA without protein are consistent with variations in the protein translation. Cases of protein without mRNA were mostly observed because of a sensitivity difference between the ISH and IHC. In conclusion, both ISH and IHC represent the increased *AIB1* gene expression with similar accuracy.

FISH of Pancreatic Tissues. Next, FISH analysis was performed on a tissue microarray to assess the *AIB1* copy number changes in a subset of cases. Diploid copy number was observed in all of the normal tissues present on the array ($n = 11$). Fig. 4*A* shows a representative example with epithelial cells of a pancreatic duct. In contrast to normal tissues, an increased copy number of the *AIB1* gene was observed in 37% of the pancreatic adenocarcinoma cores (17 of 46). In each of these 17 adenocarcinoma cores, at least 30% of the cells analyzed showed a range of *AIB1* copies between three and five copies per cell. In the 11 normal tissue cores, no increase in the number of signals was observed, and the majority of the cells with detectable FISH signal showed two copies of the gene. Pancreatic adenocarcinoma cells from one representative case with an average of four detectable gene copies per cell are shown in Fig. 4*B*. Although an increase in copy numbers did correlate with mRNA overexpression [$n = 50$, $r = 0.55$ (95% confidence interval, 0.32–0.72), $P < 0.0001$], no significant direct correlation existed with protein expression ($P > 0.2$) in the small subset investigated. We conclude from this that little over one third of pancreatic adenocarcinoma harbor an increased number of *AIB1* gene copies.

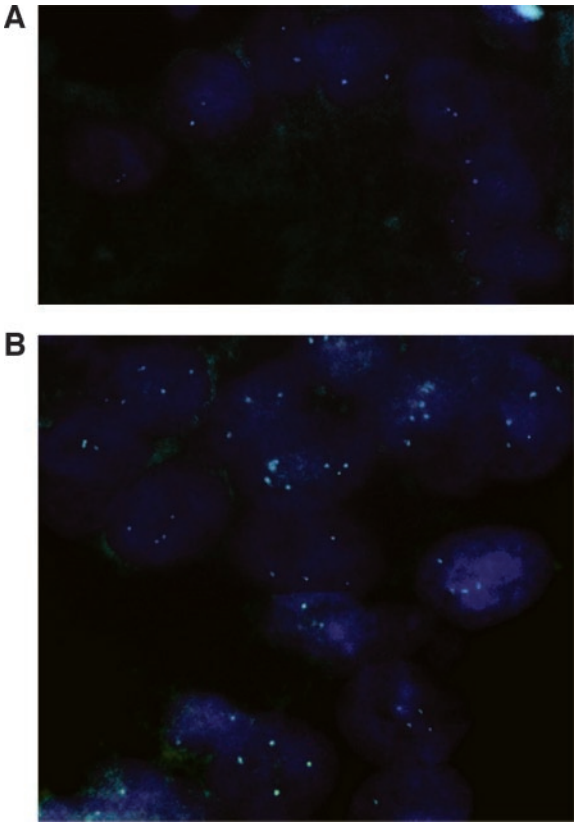

Fig. 4 FISH analysis for genomic AIB1 in tissue samples was performed using a probe consisting of DNA from the clones RP11-109C3 and RP11-456N23 (BACPAC Resources). *A*, epithelial cells of a normal pancreatic duct. *B*, pancreatic adenocarcinoma cells. 0 of 11 normal and 17 of 46 cancer samples showed increased (>2) AIB1 copy numbers in at least 30% of cells.

DISCUSSION

In this study, we show for the first time that *AIB1* is aberrantly overexpressed during progression of human pancreatic adenocarcinoma. Similar to other reported genetic aberrations (*p16*, *kras*, and *dpc4*; refs. 28, 29), we observed a progressive increase in the frequency of *AIB1* abnormalities from pancreatitis over low-grade PanIN lesions through high-grade PanIN to invasive ductal adenocarcinomas. The levels of expression (64.5% of the tumors for AIB1 protein and 73.7% for mRNA) are comparable or higher in pancreatic cancer than those that have been previously reported in breast carcinoma where high levels of mRNA expression is observed in 30 to 60% of the tumors (7, 16) and protein overexpression and gene amplification in ~10% (7, 27). Expression is also comparable with other neoplasms in which AIB1 expression has been reported, namely meningioma (30) and cancers of the prostate (12), ovaries (7), and head and neck (25). Remarkable concordance of *AIB1* mRNA and AIB1 protein expression was seen in our samples. Although the mechanisms of AIB1 overexpression in pancreatic cancer remain to be explored, we believe, based on our limited FISH data, that in a subset of cases, gene amplification may be responsible for the high expression levels.

Interestingly, AIB1 expression is almost undetectable in the normal pancreata in contrast to normal breast epithelia, where low levels of mRNA expression are seen in 30% of the cases (16). In addition, we observed in our study that AIB1 protein staining was mostly located in the nuclei of the adenocarcinoma and neoplastic PanIN cells, whereas in positive, normal breast epithelium, a heterogeneous cytoplasmic and nuclear staining pattern was observed (ref. 27 and unpublished data from our lab). On the basis of data emanating from our laboratory and other groups (31), we believe that the nuclear localization of AIB1 most likely indicates the transcriptionally

active form. Our findings suggest that the overexpression of AIB1 might confer a growth advantage to pancreatic ductal epithelial cells in the process of neoplastic transformation. Consistent with this, increased expression of AIB1 is frequent in high-grade PanIN.

The role of *AIB1* in tumorigenesis is an active area of investigation. We have shown previously that AIB1 can be rate limiting for estrogen-stimulated proliferation of breast tumors (15). Obviously, it is unlikely that the primary role of AIB1 in pancreatic cancer is related to estrogen because this receptor does not seem to play a major role in pancreatic cancer development (32). It has also been reported that AIB1 correlates with HER2/Neu overexpression in breast cancers (ref. 16 and our unpublished data), yet none of the tumors in our study was overexpressing HER2/Neu (determined during diagnostic immunohistochemistry; data not shown). However, AIB1 has a broad spectrum of nuclear receptors that it can coactivate, and it is possible that the potentiation of these might be involved in pancreatic cancer development. Recently, a number of laboratories, including ours, have determined that AIB1 is rate limiting for insulin-like growth factor I and epidermal growth factor signaling in cancer cell lines (Ref. 19 and Oh et al.[3]). This is also consistent with the *p/CIP* (mouse *AIB1*)-knockout mouse that loses responsiveness to insulin-growth factor I (18). Interestingly, the proliferation of pancreatic cancer is also known to depend highly on growth factor signaling, and a number of the receptors or ligands are overexpressed in this cancer. Insulin-like growth factor I receptor and epidermal growth factor receptor are most notable among these (33–35). It is therefore possible that clones with high levels of AIB1 expression are selected for during progression of pancreatic cancer because these might be expected to be sensitized to proliferation and invasion driven by growth factors via autocrine and/or paracrine mechanisms.

We conclude that the role of *AIB1* is not limited to hormone-sensitive tumors, namely meningioma (30) and breast (7, 27), prostate (12), and ovarian cancer (7), but that it may also be significantly involved in pancreatic cancer pathogenesis, as evidenced by the frequent overexpression of AIB1 protein and mRNA. The up-regulation of nuclear AIB1 protein and increased *AIB1* gene copy numbers in precursor lesions of pancreatic adenocarcinoma, especially high-grade lesions, hold promise as a potential diagnostic tool in small biopsy or exfoliative cytology specimens. For such samples, distinction from clinicopathological mimics such as chronic pancreatitis is critical. Because $<15\%$ of pancreatitis samples show low positive AIB1 protein staining, high levels of AIB1 protein (especially with pronounced nuclear localization) might serve as an important diagnostic indicator.

[3] A. Oh, H.-J. List, R. Reifer, et al. The nuclear receptor coactivator AIB1 mediates IGF-1–induced phenotypic changes in human breast cancer cells, submitted for publication, 2004.

ACKNOWLEDGMENTS

We thank Isaiah Fidler (University of Texas M. D. Anderson Cancer Center, Houston, TX) for making the cell lines COLO357, L3.6pl, and L3.6sl available.

REFERENCES

1. Greenlee RT, Hill-Harmon MB, Murray T, Thun M. Cancer statistics, 2001. CA - Cancer J Clin 2001;51:15–36.

2. Hruban RH, Adsay NV, Albores-Saavedra J, et al. Pancreatic intraepithelial neoplasia: a new nomenclature and classification system for pancreatic duct lesions. Am J Surg Pathol 2001;25:579–86.

3. van Heek NT, Meeker AK, Kern SE, et al. Telomere shortening is nearly universal in pancreatic intraepithelial neoplasia. Am J Pathol 2002;161:1541–7.

4. Hruban RH, Petersen GM, Goggins M, et al. Familial pancreatic cancer. Ann Oncol 1999;10 (Suppl 4):69–73.

5. Onate SA, Tsai SY, Tsai MJ, O'Malley BW. Sequence and characterization of a coactivator for the steroid hormone receptor superfamily. Science (Wash. DC) 1995;270:1354–7.

6. Voegel JJ, Heine MJS, Zechel C, Chambon P, Gronmeyer H. TIF2, a 160 kDa transcriptional mediator for the ligand dependent activation function AF-2 of nuclear receptors. EMBO J 1996;15:3667–75.

7. Anzick SL, Kononen J, Walker RL, et al. AIB1, a steroid receptor coactivator amplified in breast and ovarian cancer. Science (Wash. DC) 1997;277:965–8.

8. Chen H, Lin RJ, Schiltz RL, et al. Nuclear receptor coactivator ACTR is a novel histone acetyltransferase and forms a multimeric activation complex with P/CAF and CBP/p300. Cell 1997;90:569–80.

9. Li H, Gomes PJ, Chen JD. RAC3, a steroid/nuclear receptor-associated coactivator that is related to SRC-1 and TIF2. Proc Natl Acad Sci USA 1997;94:8479–84.

10. Takeshita A, Cardona GR, Koibuchi N, Suen C-S, Chin WW. TRAM-1, a novel 160-kDa thyroid hormone receptor activator molecule, exhibits distinct properties from steroid receptor coactivator-1. J Biol Chem 1997;272:27629–34.

11. Suen C-S, Berrodin TJ, Mastroeni R, et al. A transcriptional coactivator, steroid co-activator-3 selectively augments steroid receptor transcriptional activity. J Biol Chem 1998;273:27645–53.

12. Gnanapragasam VJ, Leung HY, Pulimood AS, Neal DE, Robson CN. Expression of RAC 3, a steroid hormone receptor co-activator in prostate cancer. Br J Cancer 2001;85:1928–36.

13. Ghadimi BM, Schrock E, Walker RL, et al. Specific chromosomal aberrations and amplification of the AIB1 nuclear receptor coactivator gene in pancreatic carcinomas. Am J Pathol 1999;154:525–36.

14. Sakakura C, Hagiwara A, Yasuoka R, et al. Amplification and overexpression of the AIB1 nuclear receptor co-activator gene in primary gastric cancers. Int J Cancer 2000;89:217–23.

15. List HJ, Lauritsen KJ, Reiter R, et al. Ribozyme targeting demonstrates that the nuclear receptor coactivator AIB1 is a rate-limiting factor for estrogen-dependent growth of human MCF-7 breast cancer cells. J Biol Chem 2001;276:23763–8.

16. Bouras T, Southey MC, Venter DJ. Overexpression of the steroid receptor coactivator AIB1 in breast cancer correlates with the absence of estrogen and progesterone receptors and positivity for p53 and HER2/neu. Cancer Res 2001;61:903–7.

17. Xu J, Liao L, Ning G, et al. The steroid receptor coactivator SRC-3 (p/CIP/RAC3/AIB1/ACTR/TRAM-1) is required for normal growth, puberty, female reproductive function, and mammary gland development. Proc Natl Acad Sci USA 2000;97:6379–84.

18. Wang Z, Rose DW, Hermanson O, et al. Regulation of somatic growth by the p160 coactivator p/CIP. Proc Natl Acad Sci USA 2000;97:13549–54.

19. Reiter R, Wellstein A, Riegel AT. An isoform of the coactivator AIB1 that increases hormone and growth factor sensitivity is overexpressed in breast cancer. J Biol Chem 2001;276:39736–41.

20. Bruns CJ, Harbison MT, Kuniyasu H, Eue I, Fidler IJ. *In vivo* selection and characterization of metastatic variants from human pancreatic adenocarcinoma by using orthotopic implantation in nude mice. Neoplasia 1999;1:50–62.

21. Maitra A, Adsay NV, Argani P, et al. Multicomponent analysis of the pancreatic adenocarcinoma progression model using a pancreatic intraepithelial neoplasia tissue microarray. Mod Pathol 2003;16:902–12.

22. Bubendorf L, Nocito A, Moch H, Sauter G. Tissue microarray (TMA) technology: miniaturized pathology archives for high-throughput in situ studies. J Pathol 2001;195:72–9.

23. Rubin MA, Dunn R, Strawderman M, Pienta KJ. Tissue microarray sampling strategy for prostate cancer biomarker analysis. Am J Surg Pathol 2002;26:312–9.

24. Haddad B, Pabon-Pena CR, Young H, Sun WH. Assignment1 of STAT1 to human chromosome 2q32 by FISH and radiation hybrids. Cytogenet Cell Genet 1998;83:58–9.

25. Cullen KJ, Newkirk KA, Schumaker LM, et al. Glutathione *S*-transferase pi amplification is associated with cisplatin resistance in head and neck squamous cell carcinoma cell lines and primary tumors. Cancer Res 2003;63:8097–102.

26. Panoskaltsis-Mortari A, Bucy RP. *In situ* hybridization with digoxigenin-labeled RNA probes: facts and artifacts. Biotechniques 1995;18:300–7.

27. List HJ, Reiter R, Singh B, Wellstein A, Riegel AT. Expression of the nuclear coactivator AIB1 in normal and malignant breast tissue. Breast Cancer Res Treat 2001;68:21–8.

28. Hruban RH, Wilentz RE, Kern SE. Genetic progression in the pancreatic ducts. Am J Pathol 2000;156:1821–5.

29. Klein WM, Hruban RH, Klein-Szanto AJ, Wilentz RE. Direct correlation between proliferative activity and dysplasia in pancreatic intraepithelial neoplasia (PanIN): additional evidence for a recently proposed model of progression. Mod Pathol 2002;15:441–7.

30. Carroll RS, Brown M, Zhang J, et al. Expression of a subset of steroid receptor cofactors is associated with progesterone receptor expression in meningiomas. Clin Cancer Res 2000;6:3570–5.

31. Qutob MS, Bhattacharjee RN, Pollari E, Yee SP, Torchia J. Microtubule-dependent subcellular redistribution of the transcriptional coactivator p/CIP. Mol Cell Biol 2002;22:6611–26.

32. Singh S, Baker PR, Poulsom R, et al. Expression of oestrogen receptor and oestrogen-inducible genes in pancreatic cancer. Br J Surg 1997;84:1085–9.

33. Koka V, Potti A, Koch M, et al. Role of immunohistochemical identification of Her-2/neu and detection of variability in overexpression in pancreatic carcinoma. Anticancer Res 2002;22:1593–7.

34. Bardeesy N, DePinho RA. Pancreatic cancer biology and genetics. Nat Rev Cancer 2002;2:897–909.

35. Stoeltzing O, Liu W, Reinmuth N, et al. Regulation of hypoxia-inducible factor-1alpha, vascular endothelial growth factor, and angiogenesis by an insulin-like growth factor-I receptor autocrine loop in human pancreatic cancer. Am J Pathol 2003;163:1001–11.

Clinical Cancer Research

Overexpression of the Nuclear Receptor Coactivator *AIB1* (*SRC-3*) during Progression of Pancreatic Adenocarcinoma

Ralf Thorsten Henke, Bassem R. Haddad, Sung Eun Kim, et al.

Clin Cancer Res 2004;10:6134-6142.